

Analysing the contributions of lower limb muscles to eccentric cycling using musculoskeletal modeling and simulation

Stefan Venter¹, Paul J. Stapley², Joel A. Walsh², Roy Cheung³ and Manish Sreenivasa¹

Abstract—Eccentric (ECC) cycling, compared to traditional concentric cycling, has been shown to improve muscle strength and neuromuscular control at a lower metabolic cost. Despite the popularity of this exercise in the sports and rehabilitation contexts, there is a gap in our knowledge of which muscles are behaving eccentrically during ECC cycling. To this end, we used a musculoskeletal model and computer simulations to calculate joint kinematics and muscle lengths during ECC cycling. Movements were recorded using 3D motion capture technology while cycling eccentrically on a custom-built semi-recumbent ergometer. The software Opensim was used to calculate joint kinematics and muscle lengths from recorded movements. We found that among the primary knee extensors, it was predominantly the Vastii muscles that acted eccentrically in the ECC cycling phase, with other lower limb muscles showing mixed eccentric/concentric activation. Additionally, the muscle force-length and force-velocity factors in the ECC phase suggest that changes to the participant's pose and pedaling speed may elicit larger active muscle forces. Our work provides an interesting application of musculoskeletal modeling to ECC cycling, and an alternative way to help understand in-vivo muscle mechanics during this activity.

I. INTRODUCTION

Lower limb ergometers have been a common instrument in physical rehabilitation for decades. Typically, such ergometers are setup to induce a concentric contraction of lower limb muscles during the “pushing” phase of pedaling. In contrast, on an eccentric (ECC) ergometer the rider is instructed to actively resist a backwards motion of motor-driven pedals [1] (Fig. 1-A,B). The underlying assumption of this mode of cycling is that the principal muscles of the lower limb that resist the backward pedal motion are being lengthened and activated simultaneously (eccentric contractions). Compared to traditional concentric cycling, ECC cycling improves knee extensor muscle strength and size at significantly lower metabolic cost as well as having other biomechanical and neuromuscular benefits [2], [3]. Past studies on this paradigm have investigated the effects of ECC cycling on cardiopulmonary function, haemodynamics, and physiology [4]. However, despite these documented benefits of ECC cycling, it is unclear to what extent the participating muscles are behaving eccentrically (i.e. activating whilst lengthening).

*This work was funded by a University of Wollongong AEGiS grant.

¹School of Mechanical, Materials, Mechatronic and Biomedical Engineering, Faculty of Engineering and Information Sciences, University of Wollongong, 2522 Wollongong, Australia manishs@uow.edu.au

²School of Medical, Indigenous and Health Sciences, Faculty of Science, Medicine and Health, University of Wollongong, 2522 Wollongong, Australia

³School of Health Sciences, Western Sydney University, 2560 Campbelltown, Australia

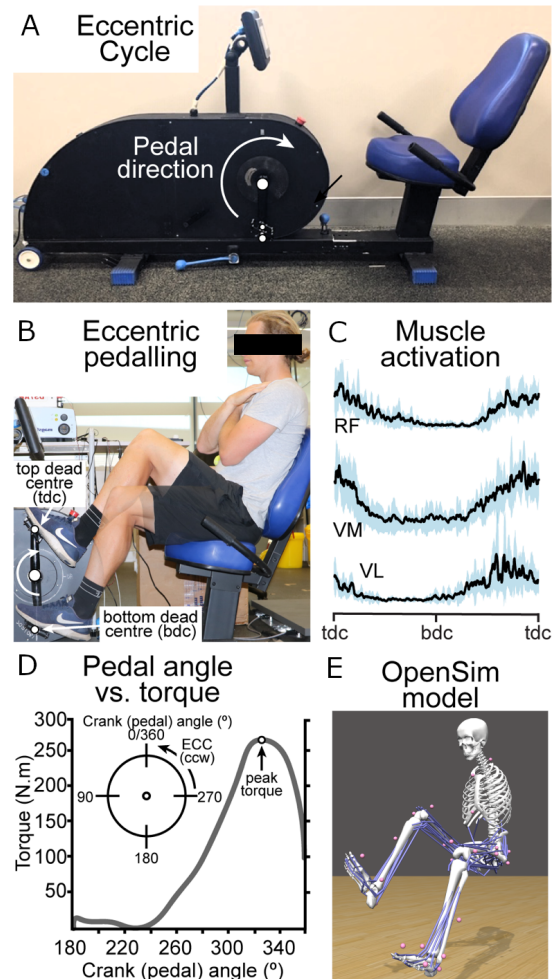


Fig. 1. (A) Semi-recumbent eccentric cycle ergometer. (B) Leg pose at the top dead center (TDC) and bottom dead center (BDC) of the pedaling action. (C) Typical recorded muscle activation signals from the Rectus Femoris (RF), Vastus Medialis (VM) and Vastus Lateralis (VL). (D) Torque applied at the pedal during part of the pedal cycle. (E) Opensim musculoskeletal model fit to the user during movements.

Recording muscle behavior in-vivo during movements is a challenging task requiring comprehensive experimental setups (e.g. the study by Peñailillo et al. [5] measuring muscle fascicle length with ultrasonography). In this context, mechanics-based models of the human musculoskeletal system can prove useful by estimating internal body parameters using computer simulations. Such models and simulation tools have been used to study the biomechanics of human movement with applications in sports, rehabilitation and surgical contexts (see [6], [7] for an overview).

In this study, we used a human musculoskeletal model to analyse the joint and muscle kinematics during cycling using a custom-built eccentric bike. Our aim was to quantify the behaviour of the principal muscles involved in the ECC cycling action throughout the pedal cycle.

II. METHODS

A. Experimental Setup and Trials

Movements of the lower limb and trunk were recorded using an 8 camera 3D motion capture system (Vicon Bonita, Vicon Motion Systems Ltd., UK) sampling at 100 Hz. A custom-built semi-recumbent stationary cycle ergometer was used to perform ECC cycling (Fig. 1, see [1] for full device details). The pedals were powered such that the user could only apply pedaling forces against the moving pedal in the ECC (opposing) phase of the pedal cycle (approx. 260°-360°, see inset Fig. 1-D).

One healthy male participant (aged 35 years, height 181.5 cm, weight 78.0 kg) with previous experience using the eccentric cycle ergometer took part in the experiment. 34 reflective markers were attached to the participant's body following the Vicon Plug-in-gait model. Following calibration trials (used for scaling the model), six pedaling trials of 90 seconds length were recorded. The first 30 seconds of each trial were required for the bike to attain a stable speed of 60 rpm, and were discarded. The last 60 seconds per trial (at constant pedal speed) were used in the analysis.

B. Musculoskeletal Model

The Gait2354 model [8] and the open-source software Opensim [6] were used to estimate the musculoskeletal kinematics of the participant during pedaling. The model contains 23 degrees of freedom and 54 lower body "line-type" muscles (Fig. 1-E). The model was first scaled to the participant's body size using the calibration trials. The scaled model was processed using the Inverse Kinematics tool that calculated the model's generalized coordinates during pedaling. Marker positions were low-pass filtered at 10Hz using a zero phase-shift double pass Butterworth filter, to minimize effects due to skin artefacts, marker vibration and electronic noise.

C. Analysis Measures

Muscle lengths and velocities were calculated from the joint kinematics using the Analyze tool in Opensim. The tool utilizes the joint angles as well as the muscle geometry (line of action of muscles as they wrap around the bone geometry) to compute the instantaneous muscle lengths during movements. The major muscles of interest for our current study were the Rectus Femoris (RF), Vastus Medialis (VM), Vastus Lateralis (VL), Vastus Intermedius (VI), Biceps Femoris (long head - BFL & short head - BFS), Semimembranosus (SM) and Semitendinosus (ST).

Hill-type muscle model equations were used to compute the force-length and force-velocity factors for each of these muscles during the motion. Note that these factors form the basis for computing muscle forces using methods such as

static optimization (e.g. [6], [9]). However, in this study we chose to focus on muscle kinematics and use the factors as an indication of the capability of the muscles to generate force, rather than estimating the actual force being generated.

Force-length factor was computed based on the equations outlined in Markowitz et al. [10] as,

$$f_{l_{CE}} = \frac{-1}{\omega^2}(\tilde{l}_{CE})^2 + \frac{2}{\omega^2}(\tilde{l}_{CE}) - \frac{1}{\omega^2} + 1 \quad (1)$$

where, $\tilde{l}_{CE} = l_{CE}/l_{opt}$, with l_{CE} the instantaneous length of the muscle contractile element, l_{opt} the optimal muscle fiber length for that muscle, and ω a parameter to adjust the shape of the force-length curve for different muscles.

Similarly, force-velocity factor was computed as per [10] as,

$$f_{v_{CE}} = \begin{cases} \frac{v_{max} + v_{CE}}{v_{max} - K v_{CE}}, v_{CE} < 0 \\ N - \frac{(N-1)(v_{max} - v_{CE})}{7.56K v_{CE} + v_{max}}, v_{CE} \geq 0 \end{cases} \quad (2)$$

where, v_{CE} was the instantaneous muscle velocity, K was a muscle-specific parameter and $v_{max} = 4.8(1 + 1.5FT)$ was the maximum contraction velocity of the muscle, with FT being the ratio of fast twitch fibres in the muscle. N was set to 1.5 for our computations as per [10]. Table I lists the parameters used to compute the $f_{l_{CE}}$ and $f_{v_{CE}}$ factors. Note that we only list the parameters of the knee extensor muscles that were of particular importance during the eccentric phase of the movement.

III. RESULTS

The inverse kinematics and muscle analysis results described in Sec. II-C were exported to and processed in MATLAB 2022a (The Mathworks Inc., Natick, MA, USA). Given the bilateral symmetry of the cycling motion, we only report the results for the right leg in the following. Data were truncated by the pedal cycle (0° to 360°) and are presented here superimposed across cycles.

A. Joint and Muscle Kinematics

Pedaling motion on the eccentric bike resulted in a range of motion in the sagittal plane between 18° to 72° for the hip, 27° to 118° for the knee and 8° to 38° for the ankle (Fig. 2-A). In the eccentric range of the pedal cycle (i.e. 260° to 360°), we observed that the hip, knee and ankle joints were in flexion. Corresponding to this joint flexion in the eccentric range, the knee extensor muscles showed a clear lengthening for the VI, VM and VL (Fig. 2-B). Interestingly, while the RF did lengthen slightly in the eccentric phase, the increase

TABLE I
MUSCLE PARAMETERS USED TO DETERMINE $f_{l_{CE}}$ AND $f_{v_{CE}}$, ADAPTED FROM [10], [11]. FIBER OPTIMAL LENGTH l_{opt} WAS BASED ON THE OPENSIM 2354 MODEL [8].

	ω	FT	K	l_{opt}
RF	0.76	0.65	9.48	0.125
VM	0.55	0.5	8.4	0.098
VI	0.55	0.5	8.4	0.095
VL	0.55	0.5	8.4	0.092

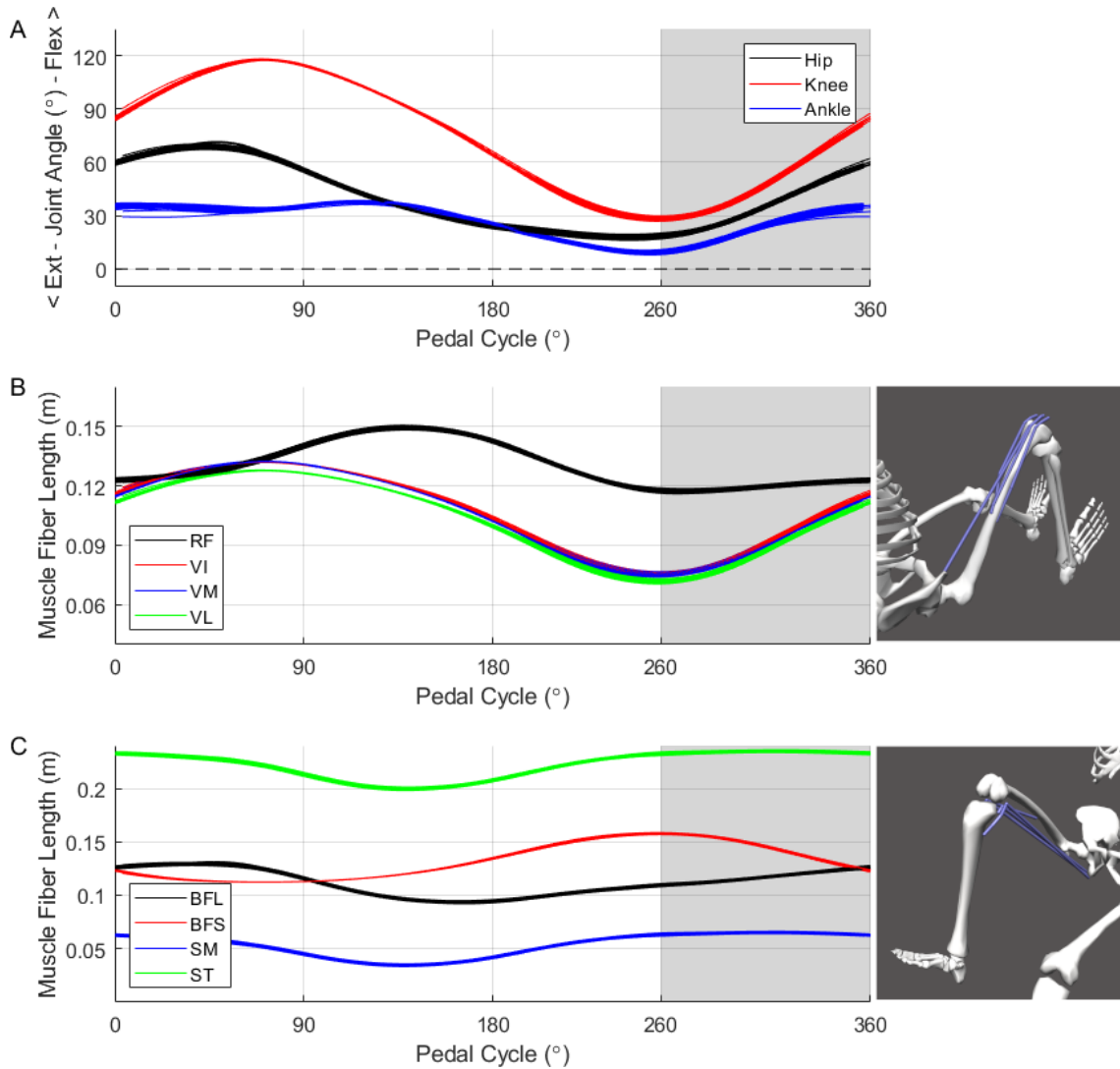


Fig. 2. Pedaling Kinematics: (A) Joint angles of the hip, knee and ankle in the sagittal plane during pedaling motion with respect to the pedal angle. Muscle fiber length of the knee extensor (B) and knee flexor (C) muscles with respect to pedal angle. Shaded region on panels indicate the eccentric range of the pedal cycle.

in length was not as pronounced as in the Vastii muscles. Muscle fiber lengths of the knee flexors (BFL & BFS, SM, ST) showed mixed results with some shortening in the ECC phase and others lengthening (Fig. 2-C).

B. Muscle Factors

Force-length factors in the ECC phase ranged from 0.77 to 1.0 for RF, VM, VI and VL (Fig. 3-A). The RF muscle was closest to its optimal length during this phase (indicated by its $f_{l_{CE}}$ value being close to 1.0), with smaller and more variable values in the Vastii muscles. Force-velocity factors on the other hand, were generally greater than 1.0 with the largest values of upto 1.3 observed in the the Vastii muscles (Fig. 3-B). The product of force-length and force-velocity factors showed a more complex behavior over the pedal cycle. In the ECC phase, this product was generally greater than 1.0 beyond a pedal angle of approximately 270° (Fig. 3-C).

IV. DISCUSSION

To our knowledge, this is the first study to use musculoskeletal modelling to analyse semi-recumbent ECC cycling. Our results suggest that, from a range of muscles in the lower limb, the Vastii (VL, VM, VI) behave eccentrically, with some other leg muscles shortening in the ECC phase (260° – 360° of pedal cycle). Therefore, some care needs to be taken when interpreting results of studies using ECC cycling that assume that the mode of muscle contraction is purely eccentric, as concentric muscular activation may also be included.

Our analysis of force-length and force-velocity factors showed that the knee extensor muscles have the capacity to generate forces in the ECC range. While the force-length factors are already in the higher range (> 0.8), even larger muscle force generation could be facilitated by optimizing the participant's configuration on the cycle ergometer such that muscle fiber lengths (especially for the Vastii muscles)

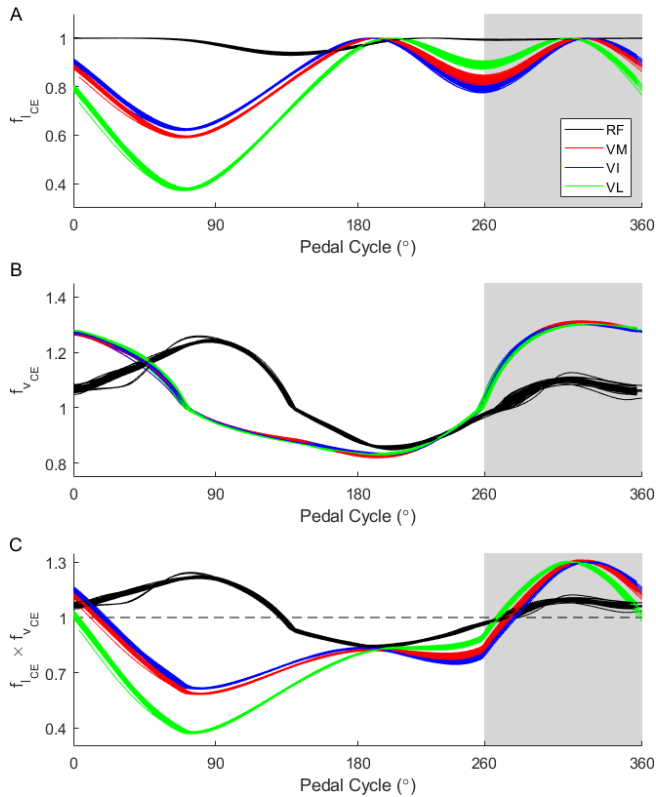


Fig. 3. Muscle Factors: (A) Muscle force-length factor (f_{lCE}) with respect to the pedal angle. (B) Muscle force-velocity factor (f_{vCE}) with respect to the pedal angle. (C) Product of muscle f_{lCE} and f_{vCE} with respect to the pedal angle. Shaded region on panels indicate the eccentric phase of the pedal cycle.

in the ECC phase are closer to the optimal fiber length.

An alternative means to increase muscle forces in the ECC phase could be to increase pedaling speed (and therefore increasing lengthening velocity). However, the ability of muscles to act as a braking force against fast lengthening [12], and the potential for damage [13] need to be considered. Fast lengthening may also induce larger forces due to muscle viscoelasticity [14]. Therefore, it may be worthwhile to investigate if further increasing these passive force contributions from the tissue rather than from voluntary muscle action, provides the additional physiological benefits resulting from ECC cycling.

The product of f_{lCE} and f_{vCE} is one of the components that determines how much force the muscle contractile element can generate in the Hill-type equation,

$$F(t) = a(t) \times f_{lCE}(t) \times f_{vCE}(t) \times F_{max} \quad (3)$$

where $a(t)$ is normalized muscle activation at time t , and F_{max} is maximum voluntary contraction force of the muscle. Our analysis illustrates how this measure ($f_{lCE} \times f_{vCE}$) can be used to gain insight into muscle function, and determine the influence of changes in muscle length and velocity on muscle force generation capacity during ECC cycling.

We note that care should be taken when interpreting this pilot study as our results are based on a single participant. We have also only modelled kinematics and not kinetics - f_{lCE} and f_{vCE} inform us about the capacity to generate force, but not if muscles are actively contributing. However, our results clearly show that the principal muscles acting eccentrically during this activity are the Vastii muscles. These findings provide a novel means for understanding the muscle contraction behavior and neuromuscular control of ECC cycling. They could also be used to explore how neuromuscular control of ECC cycling is modified by ageing or pathology, given its increasing use, in lieu of concentric cycling, in clinical settings.

REFERENCES

- [1] J. A. Walsh, D. J. McAndrew, D. J. Henness, J. Shemmel, D. Cuicuri, and P. J. Stapley, "A semi-recumbent eccentric cycle ergometer instrumented to isolate lower limb muscle contractions to the appropriate phase of the pedal cycle," *Frontiers in Physiology*, vol. 12, 2021.
- [2] L. Peñailillo, A. Blazevich, H. Numazawa, and K. Nosaka, "Metabolic and muscle damage profiles of concentric versus repeated eccentric cycling," *Medicine & Science in Sports & Exercise*, vol. 45, no. 9, pp. 1773–1781, 2013.
- [3] S. Elmer, S. Hahn, P. McAllister, C. Leong, and J. Martin, "Improvements in multi-joint leg function following chronic eccentric exercise," *Scandinavian Journal of Medicine & Science in Sports*, vol. 22, no. 5, pp. 653–661, 2012.
- [4] J. Douglas, S. Pearson, A. Ross, and M. McGuigan, "Chronic adaptations to eccentric training: A systematic review," *Sports medicine*, vol. 47, no. 5, pp. 917–941, 2017.
- [5] L. Peñailillo, A. J. Blazevich, and K. Nosaka, "Muscle fascicle behavior during eccentric cycling and its relation to muscle soreness," *Medicine & Science in Sports & Exercise*, vol. 47, no. 4, pp. 708–717, 2015.
- [6] S. L. Delp, F. Anderson, A. Arnold, P. Loan, A. Habib, C. John, E. Guendelman, and D. G. Thelen, "Opensim: Open-source software to create and analyze dynamic simulations of movement," *IEEE Trans. in Biomedical Engineering*, vol. 54, pp. 1940–1950, 2007.
- [7] F. De Groote and A. Falisse, "Perspective on musculoskeletal modelling and predictive simulations of human movement to assess the neuromechanics of gait," *Proceedings of the Royal Society B: Biological Sciences*, vol. 288, no. 1946, p. 20202432, 2021.
- [8] S. L. Delp, J. P. Loan, M. G. Hoy, F. E. Zajac, E. L. Topp, and J. M. Rosen, "An interactive graphics-based model of the lower extremity to study orthopaedic surgical procedures," *IEEE Trans. in Biomedical Engineering*, vol. 37, pp. 757–767, 1990.
- [9] M. Sreenivasa, P. Soueres, and Y. Nakamura, "On using methods from robotics to study human task dependent balance during whole-body pointing and drawing movements," in *IEEE RAS/EMBS International Conference on Biomedical Robotics and Biomechanics*, 2012, pp. 1353–1358.
- [10] J. Markowitz and H. Herr, "Human leg model predicts muscle forces, states and energetics during walking," *PLOS Comput Biol*, vol. 12, no. 5, 2016.
- [11] B. R. Umberger, "Stance and swing phase costs in human walking," *Journal of the Royal Society, Interface*, vol. 7, no. 50, pp. 1329–1340, 2010.
- [12] J. Alcazar, R. Csapo, I. Ara, and L. M. Alegre, "On the shape of the force-velocity relationship in skeletal muscles: The linear, the hyperbolic, and the double-hyperbolic," *Front Physiol*, vol. 10:769, 2019.
- [13] S. Hody, J.-L. Croisier, T. Bury, B. Rogister, and P. Leprince, "Eccentric muscle contractions: Risks and benefits," *Frontiers in Physiology*, vol. 10, 2019.
- [14] J. M. Winters, *Hill-Based Muscle Models: A Systems Engineering Perspective*. New York, NY: Springer New York, 1990, pp. 69–93.